

# Crack Identification Using Improved 2D Cracked Finite Element in Conjunction with Micro Genetic Algorithm

Aysha Kalanad<sup>1</sup>

B. N. Rao<sup>2</sup>

## Abstract

In this paper a crack diagnosis method based on an improved two-dimensional (2-D) finite element (FE) with an embedded edge crack, and micro genetic algorithm ( $\mu$ -GA) is proposed. The crack is not physically modeled within the element, but instead, its influence on the local flexibility of the structure is accounted for by the reduction of the element stiffness as a function of the crack length. The components of the stiffness matrix for the cracked element are determined from the Castigliano's first principle. The element was implemented in the commercial FE code ABAQUS as a user element (UEL) subroutine. The identification of the crack location and depth is formulated as an optimization problem, and  $\mu$ -GA is used to find the optimal location and depth by minimizing the cost function based on the difference of measured and calculated natural frequencies. The proposed crack detection procedure using the improved 2-D FE with an embedded edge crack, and  $\mu$ -GA is validated using the available experimental and FE modal analysis data reported in the existing literature. The predicted crack locations and crack sizes demonstrate that this approach is capable of detecting small crack location and depth with small errors.

**Keywords:** Cracked finite element, Micro genetic algorithm, User element, ABAQUS, Natural frequency, Crack diagnosis.

---

<sup>1</sup> MS Student, Structural Engineering Division, Indian Institute of Technology Madras, Chennai, India  
E-mail: aysha.kalanad@gmail.com

<sup>2</sup> Associate Professor, Structural Engineering Division, Indian Institute of Technology Madras, Chennai, India  
E-mail: bnrao@iitm.ac.in

# 1. Introduction

The presence of a crack in a structural member reduces the stiffness and increases the damping of the structure. As a consequence, there is a decrease in natural frequencies and modification of the modes of vibration. Several approaches have been used to model the problem of a cracked beam using the finite element method. One-dimensional cracked beam finite elements for vibration studies have been developed previously by other researchers (Krawczuk *et al.* 2003; Chondros *et al.* 2001). With an aim to simulate the crack presence without actually modeling the crack, more recently a two-dimensional cracked finite element was developed by Potirniche *et al.* (2008) for fatigue and fracture applications. However, the accuracy of the predicted natural frequency using the cracked finite element developed by Potirniche *et al.* (2008) for higher values of crack depth ratios is less.

In all the papers cited above, it was assumed that the material around the crack tip behaved in a purely elastic manner. In practice, in many materials, the plastic zone appears around the crack tip, and flexibility of the structure increases more than it is observed for a purely elastic material. Krawczuk *et al.* (2000, 2001) developed cracked beam and plate finite elements, taking into account the effect of plasticity ahead of the crack tip. These efforts used Castigliano's second theorem, which states that the displacements can be obtained by taking the partial derivatives of the strain energy with respect to the correspondingly applied forces. In a standard finite element implementation, the use of Castigliano's second theorem is not practical because the resulting singular compliance matrix must be inverted in order to obtain the element stiffness matrix.

This paper presents a crack diagnosis method based on an improved 2-D FE with an embedded edge crack, and  $\mu$ -GA. A novel two-dimensional finite element with a single, non-propagating, open embedded edge crack, which takes into account the influence of the plastic zone ahead of the crack tip on flexibility of the element, is developed. The element is implemented in the commercial finite element code ABAQUS as user element (UEL) subroutine. The identification of the crack location and depth is formulated as an optimization problem, and  $\mu$ -GA is used to find the optimal location and depth by minimizing the cost function based on the difference of measured and calculated natural frequencies.

## 2. Improved Cracked Finite Element Model

For predicting natural frequency of a cracked beam more accurately, in this section, the following improvements to the cracked FE originally developed by Potirniche *et al.* (2008) are presented: (a) to handle crack depth ratios ranging up to 0.9; and (b) the additional flexibility of the cracked element due to the applied shear forces. Consider the cracked FE with the node numbering and the degrees of freedom per node as shown in Figure 1, the mathematical definition details of which are given in Potirniche *et al.* (2008)

In Figure 1, the tensile force at node 3 gives a force and a moment, both of which contribute to an opening of the crack. Hence the contribution  $K_{IF_3}$  of the nodal force  $F_3$  at node 3 is summation of the SIFs given by the force and the resulting bending moment  $F_3 h/2$  ( $h$  is the element depth), which can be written as

$$K_{IF_3} = K_{IF_3}^f + K_{IF_3}^m, \quad (1)$$

where

$$K_{IF_3}^f = F_f \frac{F_3}{ht} \sqrt{\pi\alpha} \quad \text{and} \quad K_{IF_3}^m = F_m \frac{3F_3}{ht} \sqrt{\pi\alpha}, \quad (2)$$

with  $t$  being the element thickness.

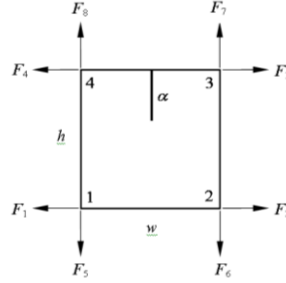


**Figure 1: Details of two-dimensional cracked finite element**

The FRANC2DL FE code (Wawrzynek and Ingraffea, 1994) is used with the  $J$ -integral option to extract the SIFs from stress strain fields around the crack tip location. 2-D FE models having  $w/h=2$  with degrees of freedom ranging from 3510 (for the case  $\alpha/h=0.1$ ) to 4258 (for the case  $\alpha/h=0.9$ ), along with a ring of six-noded quarter-point elements around the crack tip and eight-noded elements elsewhere are used under plane stress conditions. The minimum element size at the crack tip location is  $0.0025w$ . Crack length to depth ratios ( $\alpha/h$ ) are varied from 0.1 to 0.9 with nodal forces applied at various locations on the cracked element. Using the SIFs values obtained from FRANC2DL for  $\alpha/h$  ranging from 0.1 to 0.9, and Equation 2, the geometrical factors  $F_f$  and  $F_m$ , for the cracked element under tensile and bending loading respectively, are obtained by curve fitting techniques as a function of  $\alpha/h$  as follows,

$$F_f\left(\frac{\alpha}{h}\right) = 2.6233 - 51.173\frac{\alpha}{h} + 551.45\left(\frac{\alpha}{h}\right)^2 - 2563.7\left(\frac{\alpha}{h}\right)^3 + 5883.6\left(\frac{\alpha}{h}\right)^4 - 6472.2\left(\frac{\alpha}{h}\right)^5 + 2750.4\left(\frac{\alpha}{h}\right)^6, \quad (3)$$

and

$$F_m\left(\frac{\alpha}{h}\right) = 1.6426 - 18.687\frac{\alpha}{h} + 192.08\left(\frac{\alpha}{h}\right)^2 - 883.57\left(\frac{\alpha}{h}\right)^3 + 2018.3\left(\frac{\alpha}{h}\right)^4 - 2213.7\left(\frac{\alpha}{h}\right)^5 + 939\left(\frac{\alpha}{h}\right)^6. \quad (4)$$

The above given geometrical factors  $F_f$  and  $F_m$  are validated for other cases with  $w/h > 2.0$  by comparing the SIFs values obtained from FRANC2DL with those values obtained using Equation 2 in conjunction with Equations 3 and 4. The effect of  $w/h$  is found to be practically negligible for  $w/h \geq 2.0$ .

Contrary to the tensile force acting at node 3 as discussed above, in Figure 1 the nodal force  $F_2$  acting at node 2 results in a force that leads to an opening of the crack and a resolved bending moment that leads to the closing of the crack. Hence the contribution  $K_{IF_2}$  of the nodal force  $F_2$  at node 2 can be written as

$$K_{IF_2} = K_{IF_2}^f - K_{IF_2}^m, \quad (5)$$

where

$$K_{IF_2}^f = F_f \frac{F_2}{ht} \sqrt{\pi\alpha} \quad \text{and} \quad K_{IF_2}^m = F_m \frac{3F_2}{ht} \sqrt{\pi\alpha}, \quad (6)$$

with the geometrical factors  $F_f$  and  $F_m$  defined in Equations 3 and 4.

Following the procedure based on Castigliano's first theorem, outlined in Potirniche *et al.* (2008) the stiffness components  $K_{2j}$  and  $K_{3j}$  can be obtained using the geometrical factors  $F_f$  and  $F_m$  defined in Equations 3 and 4. The stiffness components  $K_{1j}$  and  $K_{4j}$  can also be obtained following the same procedure to that for the stiffness components  $K_{2j}$  and  $K_{3j}$ .

In Figure 1 the nodal force  $F_6$  acting at node 2 gives a shear force and a moment ( $Fw$ ), both of which contribute to mode I and II SIFs, which can be written as

$$K_{IF_6} = F_I \frac{6Fw}{h^2t} \sqrt{\pi\alpha} \quad \text{and} \quad K_{IIF_6} = F_{II} \frac{F}{ht} \sqrt{\pi\alpha}. \quad (7)$$

Using the SIFs values obtained from FRANC2DL for  $\alpha/h$  ranging from 0.1 to 0.9, and Equation 7, the geometrical factors for the cracked element  $F_I$  and  $F_{II}$  respectively, are obtained by curve fitting techniques as a function of  $\alpha/h$  as follows,

$$F_I \left( \frac{\alpha}{h} \right) = 0.821 - 9.344 \frac{\alpha}{h} + 96.04 \left( \frac{\alpha}{h} \right)^2 - 441.78 \left( \frac{\alpha}{h} \right)^3 + 1009.15 \left( \frac{\alpha}{h} \right)^4 - 1106.85 \left( \frac{\alpha}{h} \right)^5 + 469.5 \left( \frac{\alpha}{h} \right)^6, \quad (8)$$

and

$$F_{II} \left( \frac{\alpha}{h} \right) = 1.018 - 17.794 \frac{\alpha}{h} + 162.7 \left( \frac{\alpha}{h} \right)^2 + 596.45 \left( \frac{\alpha}{h} \right)^3 + 1098.3 \left( \frac{\alpha}{h} \right)^4 - 994.94 \left( \frac{\alpha}{h} \right)^5 + 353.26 \left( \frac{\alpha}{h} \right)^6. \quad (9)$$

The stiffness components  $K_{6j}$  can be obtained adopting the following procedure. Using Castigliano's first theorem, the difference between the nodal forces in the cracked ( $F_i$ ) and undamaged ( $F_i^0$ ) cases can be obtained by taking the partial derivatives of the SIFs with respect to the corresponding displacements ( $u_i$ ) by the relation,

$$F_6^0 - F_6 = \frac{2t}{E'} \left[ \int_0^\alpha K_I \frac{\partial K_I}{\partial u_6} da + \int_0^\alpha K_{II} \frac{\partial K_{II}}{\partial u_6} da \right], \quad (10)$$

where  $E' = E$  for plane stress,  $E' = E/(1-\nu^2)$  for plane strain,  $E$  and  $\nu$  are the modulus of elasticity and Poisson's ratio respectively. Replacing the SIFs in the above equation with their respective formulas in Equation 7 and after some simplifications, one obtains,

$$F_6^0 - F_6 = \frac{2\pi}{E'h^2t} \left[ \frac{36w^2}{h^2} \int_0^\alpha aF_I^2 da + \int_0^\alpha aF_{II}^2 da \right] F_6 \frac{\partial F_6}{\partial u_6}, \quad (11)$$

Defining  $A_{66}$  as,

$$A_{66} = \frac{2\pi}{E'h^2t} \left[ \frac{36w^2}{h^2} \int_0^\alpha aF_I^2 da + \int_0^\alpha aF_{II}^2 da \right], \quad (12)$$

and noting that

$$\frac{\partial F_6}{\partial u_6} = K_{66}, \quad (13)$$

the relation between the two nodal forces for the undamaged and cracked elements becomes

$$F_6^0 = (1 + A_{66}K_{66}) F_6. \quad (14)$$

Using  $\{F^0\} = [K^0]\{u\}$ , Equation 14 can be written as

$$\sum_{j=1}^8 K_{6j}^0 u_j = \sum_{j=1}^8 (1 + A_{66}K_{66}) K_{6j} u_j, \quad (15)$$

which is valid only if the coefficients multiplying the independent variables  $u_j$  on both sides of the above equation are equal,

$$K_{6j}^0 = (1 + A_{66}K_{66}) K_{6j} \quad \text{for } j=1, 2, \dots, 8. \quad (16)$$

Solving Equation 16 for  $K_{6j}$  the solution is found to be

$$K_{66} = \frac{-1 + \sqrt{1 + 4A_{66}K_{66}^0}}{2A_{66}}, \quad (17)$$

and

$$K_{6j} = \frac{2K_{6j}^0}{1 + \sqrt{1 + 4A_{66}K_{66}^0}} \quad \text{for } j=1, 2, \dots, 8 \text{ and } j \neq 6. \quad (18)$$

Similar formulas can be obtained for all the components  $K_{5j}$ ,  $K_{7j}$  and  $K_{8j}$ .

### 3. Crack identification technique

#### 3.1 Selection of variables and objective/fitness function

The  $\mu$ -GA begins by defining a chromosome, i.e. an array of variables whose values are to be optimized. In our case study the chromosome has two variables, the crack depth ratio ( $\alpha/H$ ) (the ratio of the crack depth ( $\alpha$ ) to the beam height ( $H$ )) and crack location ratio ( $c/L$ ) (the ratio of the crack location ( $c$ ) to the beam length ( $L$ )). Thus we have:

$$\text{Chromosome} = [\text{Cracked element number, Crack depth ratio}]. \quad (19)$$

Once a particular chromosome is defined, using the decoded values of the cracked element number and crack depth ratio ( $\alpha/H$ ), the ABAQUS input file for modal analysis is generated by inserting the improved 2-D FE into the mesh at the location defined by cracked element number. Based on the computed natural frequencies from modal analysis using ABAQUS, the objective/fitness function to be minimized is defined as follows:

$$F(\text{Cracked element number, } \alpha/H) = \sum_{i=1}^n \left| \omega_c / \omega_i - \omega_c / \omega_i^* \right|, \quad (20)$$

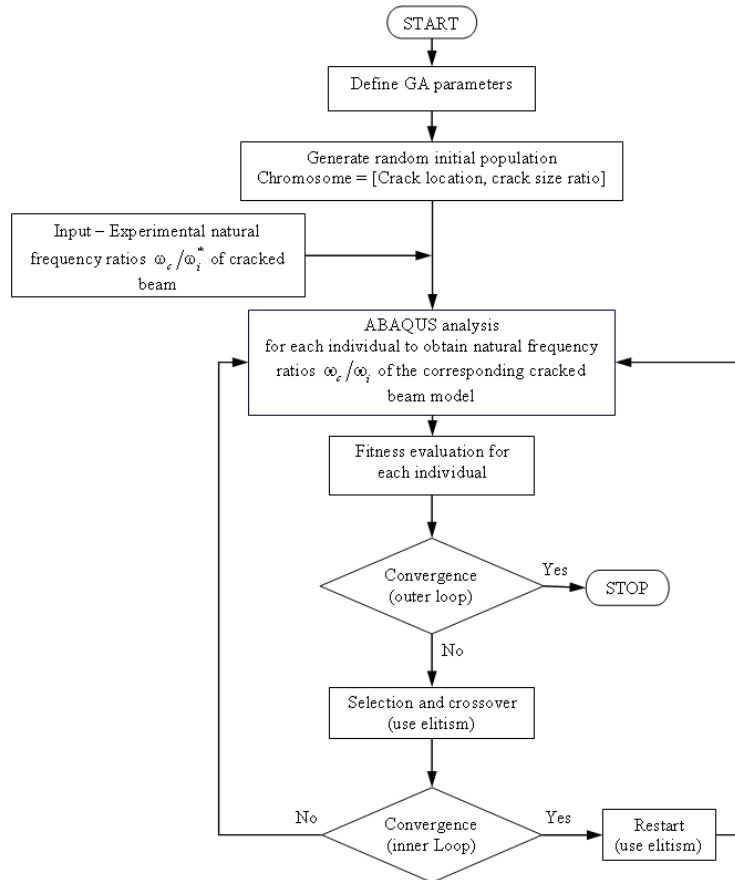


Figure 2: Flowchart of Micro-GA based crack detection method

where  $n$  is the number of frequency ratios being considered,  $\omega_c/\omega_i$  are the natural frequency ratios, which are functions of the cracked element number and crack depth ratio ( $\alpha/H$ ), and are calculated using the improved 2-D FE, and  $\omega_c/\omega_i^*$  are the natural frequency ratios determined through modal analysis experiments, which are applied to the crack detection system as inputs (see Figure 2).

### 3.2 Chromosome size and encoding

Instead of the standard uniform discretization of the possible interval of the cracked element number and crack depth ratio ( $\alpha/H$ ), they will be assumed to take one value among a discrete set of values in the possible interval. This is done in order to reduce the search space and also to bias the search away from regions of the search space where they assume unrealistic values.

Crack location and crack depth parameters can be an integer in the range  $1-2^n$  and  $1-2^m$  respectively, with  $n$  and  $m$  being the number of bits used to encode each possible value of the cracked element number and crack depth ratio ( $\alpha/H$ ). Crack location and crack depth parameters correspond to an entry in the tables of possible values for the cracked element number and crack depth ratio ( $\alpha/H$ ). The tables are built preserving an ordering of increasing crack location ratio ( $c/L$ ) and crack depth ratio ( $\alpha/H$ ), e.g. integer 1 represents less crack location ratio/crack depth ratio than integer 2 and so on. The tables are built according to a recurrent formula. In this way, one fixes the crack location ratio ( $c/L$ ) and crack depth ratio ( $\alpha/H$ ) for the first integer and the next values are increased as follows:

$$\frac{c}{L}(i) = \frac{c}{L}(i-1) + \Delta \frac{c}{L}, \quad i = 2, \dots, 2^m, \quad (21)$$

$$\frac{\alpha}{H}(i) = \frac{\alpha}{H}(i-1) + \Delta \frac{\alpha}{H}, \quad i = 2, \dots, 2^n, \quad (22)$$

where  $\Delta c/L$  and  $\Delta \alpha/H$  are the increment of crack location ratio ( $c/L$ ) and crack depth ratio ( $\alpha/H$ ) respectively, for each element of the tables. The values of  $\Delta c/L$  and  $\Delta \alpha/H$  are by the user according to the characteristics of the problem at hand, the available prior information (such as the maximum expected level of the crack location ratio ( $c/L$ ) and crack depth ratio ( $\alpha/H$ )), and the values  $n$  and  $m$  adopted. If the exact value of the real crack location ratio ( $c/L$ ) and crack depth ratio ( $\alpha/H$ ) occurring in the structure is not represented in the tables, the  $c/L$  and  $\alpha/H$  should go to the closest value of the respective tables. During the search if the crack location and crack depth parameter values falls out of the respective possible entry values in the tables, their values needs to be adjusted or reassigned to an entry in the tables corresponding to  $\text{INT}(\text{possible range} \times \text{a uniform random number generated between 0 and 1})$ . An individual chromosome is thus a vector of integers (binary encoded) representing a candidate solution that corresponds to a cracked element number and crack depth ratio ( $\alpha/H$ ).

### 3.3 Initial population

In order to determine the appropriate population size in this study, the various population sizes of 5, 8, 10, 12 and 15 individuals, each represented by a vector generated at random, are tested. The experience gained in the convergence study is used to analyze the problems presented in the numerical example.

### 3.4 Objective/fitness function evaluation

Natural frequencies are obtained through ABAQUS modal analysis in conjunction with the improved 2-D FE, and the objective/fitness function is evaluated for each chromosome, decoded values of which represent the cracked element number and crack depth ratio ( $\alpha/H$ ).

### 3.5 Convergence criterion

Overall convergence criterion is checked. If the criterion is satisfied, the whole iteration process is stopped; otherwise, continue to the next step. In this study the total prescribed number of generations (= 200) is the overall convergence criterion, and the global algorithm stops when the prescribed number of generations is reached (outer loop).

### 3.6 Reproduction and iterating the algorithm

The population for the next generation is obtained through tournament selection and uniform crossover with a crossover rate of 1.0. The elitism strategy is applied to preserve the best members. Inner loop nominal convergence is checked. If the inner loop does not converge, repeat steps (3.4) to (3.6). Otherwise, restart and regenerate (replacing the discarded chromosomes in the population by new chromosomes) a new population randomly while keeping the best individual from the previous generation. This replacement of the entire population is for searching the overall space for better solutions in  $\mu$ -GA. Repeat steps (3.4) to (3.6).

## 4. Numerical Example

Patil and Maiti (2003) reported natural frequencies obtained by FE analysis of uniform beams with two cracks on three pin supports, starting from one of the simply supported ends. The crack depth was varied from  $0.1H$  to  $0.5H$  (the depth of the beam,  $H = 0.02m$ ). Uniform beam on three pin supports model was made of cross-sectional area  $0.02m \times 0.012m$  with a length of each span  $0.3m$ . It had the following material properties: Young's modulus  $E = 210 \times 10^9 N/m^2$ , density  $\rho = 7860 kg/m^3$ , the Poisson ratio  $\nu = 0.3$ .



Each span of the uniform beam is modeled with 59 standard four node elements ABAQUS elements and one UEL at the top of the beam. Typical discretization of uniform beam is shown in Figure 3. For the discretization shown in Figure 3, the possible values of the cracked element number are 60 i.e. considering one crack in each span the possible value of the cracked element number for the first and second crack is between 61–90 and 91–120 respectively. For the crack depth ratio ( $\alpha/H$ ),  $2^5$  possible values in the interval  $0 < \alpha/H < 0.5$  with an increment of  $\Delta\alpha/H = 0.5/32$  are considered. So the cracked element number requires 5 bits, and the crack depth ratio ( $\alpha/H$ ) requires 5 bits, and thus every individual chromosome for uniform beam with two normal edge cracks contains  $2 \times 10 = 20$  bits.

The method for crack identification is verified for several combinations of crack locations and crack sizes listed in Table. 1. The predicted crack locations and crack sizes are in good agreement with the actual values with the average error in the crack location and crack size predictions equal to 1.15 and 3.59 respectively.

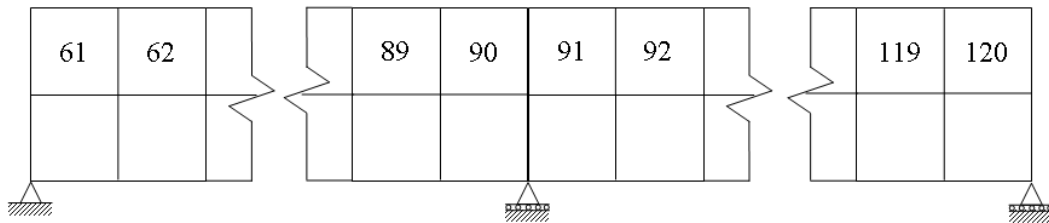


**Figure 3: Discretization of uniform beam with candidate cracked elements in top layer**

**Table 1: Comparison of predicted crack positions and sizes of uniform beam with corresponding actual values**

Crack case		Actual crack (Patil and Maiti, 2003)		Predicted crack		Predicted error (%)	
		Location $c/L$	Size $\alpha/H$	Location $c/L$	Size $\alpha/H$	Location $c/L$	Size $\alpha/H$
1	Crack 1	0.250	0.250	0.242	0.266	0.83	1.56
	Crack 2	0.750	0.150	0.742	0.141	0.83	0.94
2	Crack 1	0.250	0.250	0.258	0.281	0.83	3.13
	Crack 2	0.750	0.250	0.758	0.266	0.83	1.56
3	Crack 1	0.250	0.250	0.258	0.188	0.83	6.25
	Crack 2	0.750	0.350	0.758	0.422	0.83	7.19
4	Crack 1	0.250	0.250	0.258	0.328	0.83	7.81
	Crack 2	0.750	0.500	0.758	0.500	0.83	0.00
5	Crack 1	0.300	0.150	0.325	0.141	2.50	0.94
	Crack 2	0.600	0.250	0.592	0.266	0.83	1.56
6	Crack 1	0.350	0.250	0.358	0.203	0.83	4.69
	Crack 2	0.600	0.300	0.608	0.375	0.83	7.50
7	Crack 1	0.400	0.350	0.392	0.406	0.83	5.63
	Crack 2	0.700	0.350	0.708	0.375	0.83	2.50
8	Crack 1	0.450	0.150	0.475	0.094	2.50	5.63
	Crack 2	0.650	0.150	0.625	0.156	2.50	0.63

## 5. Conclusions

This paper presents an improved 2-D FE with an embedded edge crack for crack depth ratios ranging up to 0.9 and for predicting natural frequency of a cracked beam more accurately. The FRANC2DL FE code is used with the  $J$ -integral option to extract the stress intensity factors from stress strain fields around the crack tip location. The geometric factors for various loading cases of the cracked element for crack depth ratios ranging up to 0.9 are obtained by means of curve fitting techniques, and they are subsequently used to obtain the components of the stiffness matrix for the cracked element from the Castigliano's first theorem using fracture mechanics concepts. The element is implemented in the commercial FE code ABAQUS as user element subroutine.  $\mu$ -GA based crack identification methodology to detect crack location and size in conjunction with the improved cracked element is also presented for singularity problems like a cracked beam. The proposed  $\mu$ -GA based crack detection procedure using the improved 2-D FE is validated using the available experimental and FE modal analysis data reported in the existing literature. The predicted crack locations and crack sizes are in good agreement with the actual values. Future work will attempt to extend this approach to account for the influence of the plastic zone ahead of the crack tip on flexibility of structures.

## References

- Krawczuk M, Palacz M and Ostachowicz W (2003) "The dynamic analysis of a cracked Timoshenko beam by the spectral element method." *Journal of Sound and Vibration*, **264**: 1139–1153.
- Chondros TG, Dimarogonas AD and Yao J (2001) "Vibration of a beam with a breathing crack." *Journal of Sound and Vibration*, **239**: 57–67.
- Potirniche GP, Hearndon J, Daniewicz SR, Parker D, Cuevas P, Wang PT and Horstemeyer MF (2008) "A two-dimensional damaged finite element for fracture applications." *Engineering Fracture Mechanics*, **75**: 3895–3908.
- Krawczuk M, Żak A and Ostachowicz W (2000) "Elastic beam finite element with a transverse elasto-plastic crack." *Finite Elements in Analysis and Design*, **34**: 61–73.
- Krawczuk M, Żak A and Ostachowicz W (2001) "Finite element model of plate with elasto-plastic through crack." *Computers & Structures*, **79**: 519–532.
- Wawrzynek PA and Ingraffea AR (1994) "FRANC2D: Two-dimensional crack propagation simulator, Version 2.7 User's Guide." NASA CR 4572.
- Patil DP and Maiti SK (2003) "Detection of multiple cracks using frequency measurements." *Engineering Fracture Mechanics*, **70**(12): 1553–1572.